**Supporting Information for**

# Inversion of Configuration at the Metal in Diastereomeric Imido Alkylidene Monoalkoxide Monopyrrolide (MAP) Complexes of Molybdenum

by

Smaranda C. Marinescu,[‡] Richard R. Schrock, [‡]* Bo Li,[†] and Amir H. Hoveyda[†]

[‡]Department of Chemistry 6-331, Massachusetts Institute of Technology, Cambridge, Massachusetts 02139;

[†]Department of Chemistry, Merkert Chemistry Center, Boston College, Chestnut Hill, Massachusetts 02467

**General.** All manipulations of air and moisture sensitive materials were conducted under a nitrogen atmosphere in a Vacuum Atmospheres drybox or on a dual-manifold Schlenk line. The glassware, including NMR tubes were oven-dried prior to use. Ether, pentane, toluene, dichloromethane, toluene and benzene were degassed with dinitrogen and passed through activated alumina columns and stored over 4 Å Linde-type molecular sieves. Dimethoxyethane was vacuum distilled from a dark purple solution of sodium benzophenone ketyl, and degassed three times by freeze-pump-thaw technique. The deuterated solvents were dried over 4 Å Linde-type molecular sieves prior to use. $^1H$, $^{13}C$ spectra were acquired at room temperature unless otherwise noted using Varian spectrometers and referenced to the residual $^1H/^{13}C$ resonances of the deuterated solvent ($^1H$: $CDCl_3$, δ 7.26; $C_6D_6$, δ 7.16; $CD_2Cl_2$, δ 5.32; $CD_3CN$, δ 1.94; THF-$d_8$, δ 3.58, 1.73; $C_7D_8$, δ 7.09, 7.00, 6.98, 2.09; Pyridine-$d_5$, δ 8.74, 7.58, 7.22. $^{13}C$: $CDCl_3$, δ 77.23; $C_6D_6$, δ 128.39; $CD_2Cl_2$, δ 54.00; $CD_3CN$, δ 118.69, 1.39; THF-$d_8$, δ 67.57, 25.37; $C_7D_8$, δ 137.86, 129.24, 128.33, 125.49, 20.4; Pyridine-$d_5$, δ 150.35, 135.91, 123.87) and are reported as parts per million relative to tetramethylsilane. $^{15}N$ NMR spectra were referenced externally to neat $CH_3C^{15}N$ (δ 245 ppm) in comparison to liquid $^{15}NH_3$ (δ 0 ppm).[i] $^{31}P$ NMR spectra were referenced externally to phosphoric acid 85% (δ 0 ppm). Elemental analyses were performed by Midwest Microlab, Indianapolis, Indiana.

(*R*)-**1H**,[ii] (*S*)-**2**,[ii] (*R*)-**2**,[iii] and Mo(NAr)($^{13}$CHCMe$_3$)(OTf)$_2$(dme)[iv] were prepared as described in the literature.

(*R*)-**2**(PMe$_3$). Trimethylphosphine (150 μL, 1.411 mmol, 15 equiv) was added to a solution of pure (*S*)-**2** (100 mg, 0.094 mmol, 1 equiv) in pentane (1 mL). The solution was stored at 22 °C overnight. Red crystals of a phosphine adduct (81 mg) were isolated (75% yield): $^1H$ NMR (500 MHz, $CD_2Cl_2$, 0 °C) selected peak δ 13.57 (d, 1H, *syn* Mo=C*H*, $J_{CH}$ = 122 Hz, $J_{HP}$ = 7 Hz) (Figure 1); $^1H$ NMR (500 MHz, $C_7D_8$, -30 °C) selected peak δ 13.83 (d, 1H, *syn* Mo=C*H*, $J_{CH}$ = 122 Hz, $J_{HP}$ = 7 Hz); $^{31}P$ NMR (202 MHz, $C_7D_8$, -30 °C) δ -11.5. Anal. calcd for $C_{57}H_{79}Br_2MoN_2O_2PSi$: C, 60.10; H, 6.99; N, 2.46; Found: C, 60.32; H, 7.10; N, 2.65.

X-Ray quality crystals were grown from pentane at 20 °C.

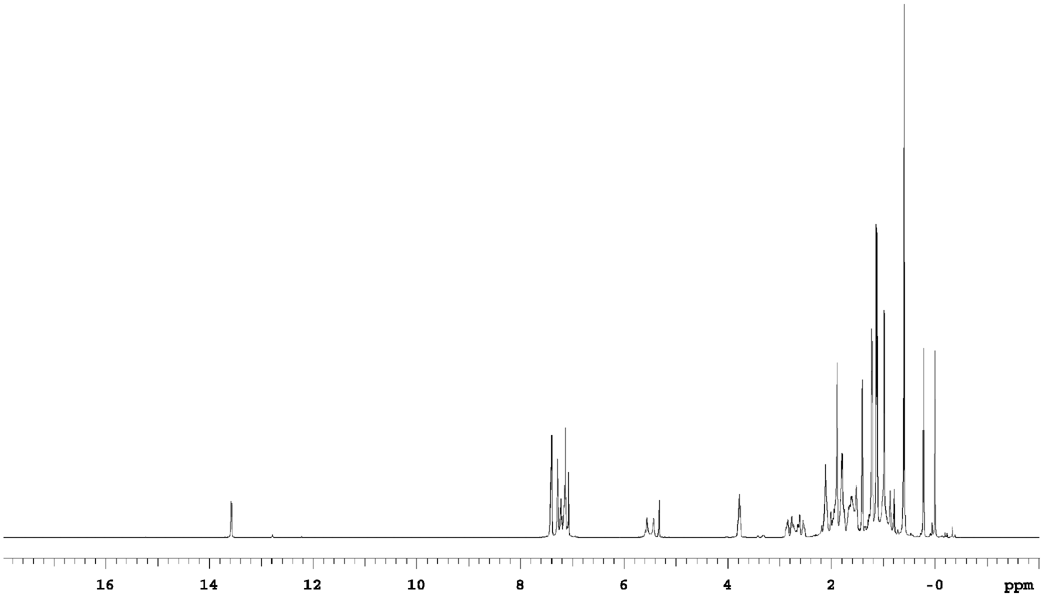

**Figure 1**. 500 MHz $^{1}$H NMR spectrum of (*R*)-**2**(PMe$_3$) in CD$_2$Cl$_2$ at 0 °C (10 mM).

## Kinetic Experiments

*Kinetic Studies in the presence of PMe$_3$ (10 mM) in C$_6$D$_6$ at 40 °C*

Solid (*R*)-**2**(PMe$_3$) (9.1 mg, 0.008 mmol) was placed in a J. Young tube. C$_6$D$_6$ (0.8 mL ) were added to the NMR tube via syringe. Reaction progress was monitored by $^{1}$H NMR spectroscopy at 40 °C, where integral areas of the alkylidene protons of (*S*)-**2** (δ 12.42 ppm, s, 1H, *syn* Mo=C*H*, $J_{CH}$ = 118 Hz), and (*R*)-**2** (δ 12.90 ppm, s, 1H, *syn* Mo=C*H*, $J_{CH}$ = 122 Hz) relative to the aromatic protons of anthracene internal standard (δ 8.16 ppm, s, 2H) were obtained at 20 minute intervals (Figure 2). The experiment was concluded when the equilibrium was reached ($K_{eq}$ = [(*S*)-**2**]/[(*R*)-**2**] = 2.0 in C$_6$D$_6$ at 40 °C). The same behavior (same $K_{eq}$, and same $k_{obs}$) was observed when a mixture of (*S*)-**2** and 1 equiv of PMe$_3$ (stock solution) was heated to 40°C.

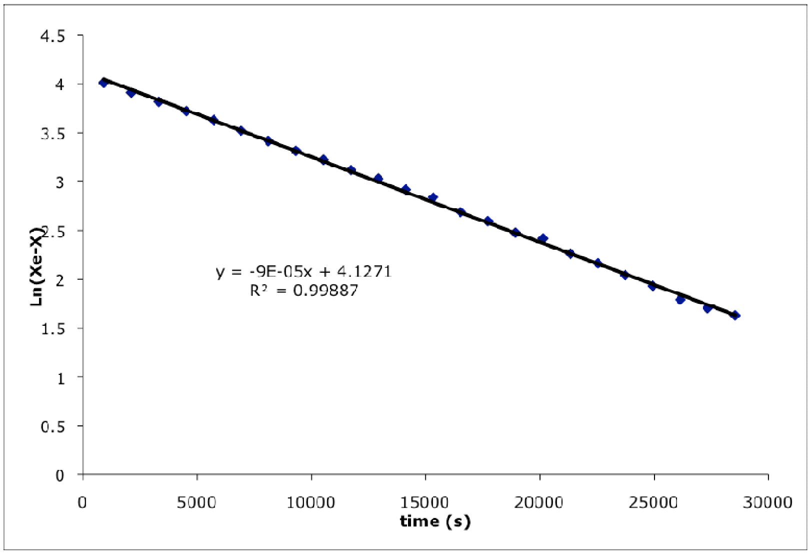

**Figure 2**. Kinetic studies for conversion of (*R*)-**2** to (*S*)-**2** in the presence of $PMe_3$ (10 mM) in $C_6D_6$ followed by $^1H$ NMR spectroscopy at 40 °C. ($X_e$ is the equilibrium concentration of (*S*)-**2**, while X is the increasing concentration of (*S*)-**2** with time.)

*Determination of order in* $PMe_3$

Solid (*R*)-**2**($PMe_3$) (9.1 mg, 0.008 mmol) was placed in a J. Young tube. A stock solution of $PMe_3$ in $C_6D_6$ was added, where appropriate, to the NMR tube via syringe to reach a total concentration of $PMe_3$ of 10 mM, 20 mM, 30 mM, 40 mM, and 50 mM, respectively. The total volume of the reaction mixture was 0.8 mL. Reaction progress was monitored by $^1H$ NMR spectroscopy at 40 °C, where integral areas of the alkylidene protons of (*S*)-**2** (δ 12.42 ppm, s, 1H, *syn* Mo=C*H*, $J_{CH}$ = 118 Hz), and (*R*)-**2** (δ 12.90 ppm, s, 1H, *syn* Mo=C*H*, $J_{CH}$ = 122 Hz) relative to the aromatic protons of anthracene internal standard (δ 8.16 ppm, s, 2H) were obtained at 20, 10, 8, 6, and 4 minute intervals, respectively. The experiments were concluded when the equilibrium was reached ($K_{eq}$ = [(*S*)-**2**]/[(*R*)-**2**] = 2.0 in $C_6D_6$ at 40 °C). The dependence of the reaction rate on the concentration of $PMe_3$ was measured at a constant total concentration of [Mo] = 10 mM. Figure 3 shows that the approach to equilibrium depends on $PMe_3$ concentration to the first order.

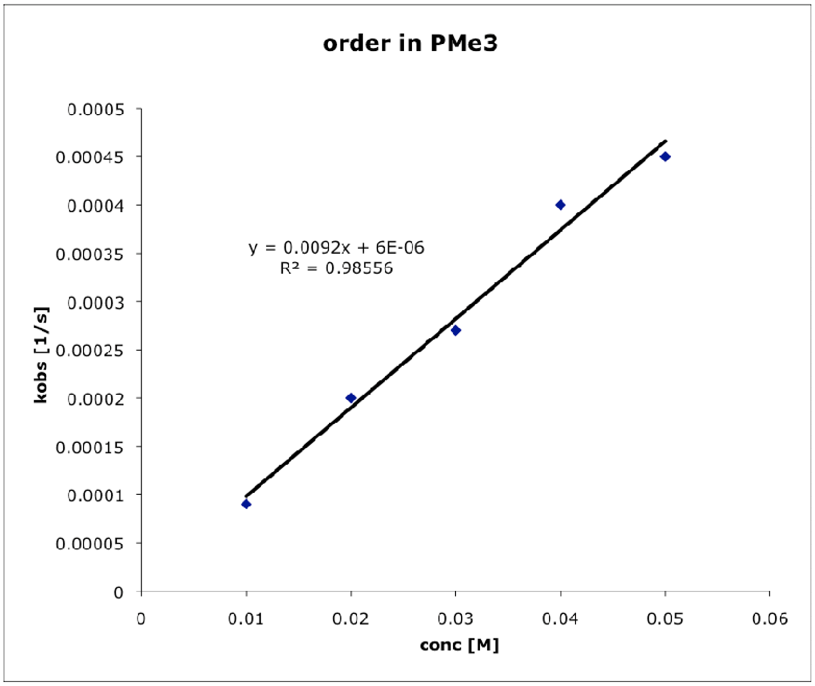

**Figure 3**. The first-order dependence of the reaction rate on the concentration of $PMe_3$.

*Kinetic Studies in the presence of $PMe_3$ (10 mM) in THF-$d_8$ at 40 °C*

Solid (*R*)-**2**($PMe_3$) (9.1 mg, 0.008 mmol) was placed in a J. Young tube. THF-$d_8$ (0.8 mL ) was added to the NMR tube via syringe. Reaction progress was monitored by $^1$H NMR spectroscopy at 40 °C, where integral areas of the alkylidene protons of (*S*)-**2** (δ 12.30 ppm, s, 1H, *syn* Mo=C*H*, $J_{CH}$ = 118 Hz), and (*R*)-**2** (δ 12.71 ppm, s, 1H, *syn* Mo=C*H*, $J_{CH}$ = 122 Hz) relative to the aromatic protons of anthracene internal standard (δ 8.44 ppm, s, 2H) were obtained at 10 minute intervals (Figure 4). The experiment was concluded when the equilibrium was reached ($K_{eq}$ = [(*S*)-**2**]/[(*R*)-**2**] = 2.0 in THF-$d_8$ at 40 °C).

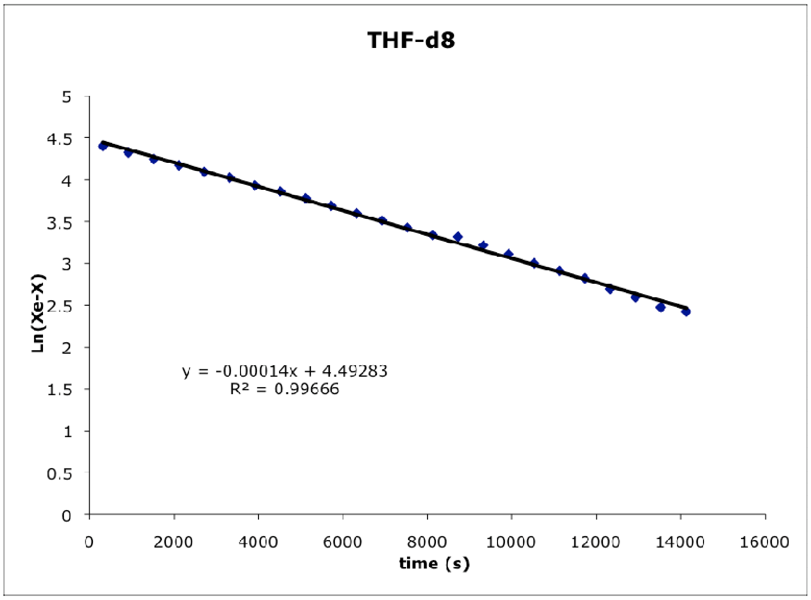

**Figure 4**. Kinetic studies for conversion of (*R*)-**2** to (*S*)-**2** in the presence of $PMe_3$ (10 mM) in THF-$d_8$ followed by $^1$H NMR spectroscopy at 40 °C. ($X_e$ is the equilibrium concentration of (*S*)-**2**, while X is the increasing concentration of (*S*)-**2** with time.)

*Kinetic Studies in the presence of $PMe_3$ (10 mM) in 1:1 $CD_3CN$:$C_6D_6$ at 40 °C*

Solid (*R*)-**2**($PMe_3$) (9.1 mg, 0.008 mmol) was placed in a J. Young tube. 0.4 mL $C_6D_6$ and 0.4 mL $CD_3CN$ were added to the NMR tube via syringe. Reaction progress was monitored by $^1$H NMR spectroscopy at 40 °C, where integral areas of the alkylidene protons of (*S*)-**2** (δ 12.81 ppm, s, 1H, *syn* Mo=C*H*, $J_{CH}$ = 118 Hz), and (*R*)-**2** (δ 13.38 ppm, s, 1H, *syn* Mo=C*H*, $J_{CH}$ = 122 Hz) relative to the aromatic protons of anthracene internal standard (δ 8.16 ppm, s, 2H) were obtained at 10 minute intervals (Figure 5). The experiment was concluded when the equilibrium was reached ($K_{eq}$ = [(*S*)-**2**]/[(*R*)-**2**] = 0.8 in 1:1 $CD_3CN$:$C_6D_6$ at 40 °C).

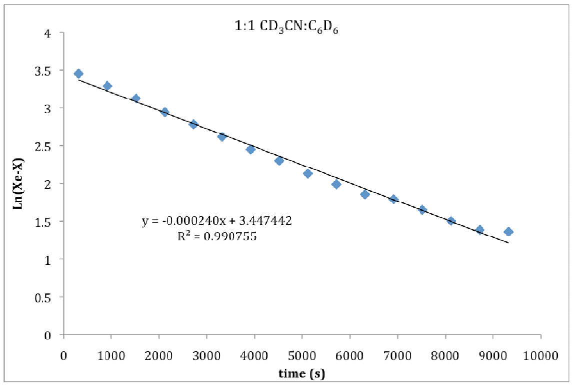

**Figure 5**. Kinetic studies for the conversion of (*R*)-**2** to (*S*)-**2**, in the presence of $PMe_3$ (10 mM) in 1:1 $CD_3CN$:$C_6D_6$ followed by $^1$H NMR spectroscopy at 40 °C. ($X_e$ is the equilibrium concentration of (*S*)-**2**, while X is the increasing concentration of (*S*)-**2** with time.)

*Kinetic Studies in the presence of $PMe_2Ph$ (1M) in $C_6D_6$ at 40 °C*

$PMe_2Ph$ (114 µL, 0.8 mmol, 100 equiv) was added via syringe to a solution of (*S*)-**2** (8.5 mg, 0.008 mmol) in $C_6D_6$. The total volume of the reaction mixture was 0.8 mL. The reaction mixture was then transferred to a J. Young tube. Reaction progress was monitored by $^1$H NMR spectroscopy at 40 °C, where integral areas of the alkylidene protons of (*S*)-**2** (δ 12.36 ppm, s, 1H, *syn* Mo=C*H*, $J_{CH}$ = 118 Hz), and (*R*)-**2** (δ 12.85 ppm, s, 1H, *syn* Mo=C*H*, $J_{CH}$ = 122 Hz) relative to the aromatic protons of anthracene internal standard (δ 8.16 ppm, s, 2H) were obtained at 20 minute intervals (Figure 6). The experiment was concluded when the equilibrium was reached ($K_{eq}$ = [(*S*)-**2**]/[(*R*)-**2**] = 2.0 in $C_6D_6$ at 40 °C).

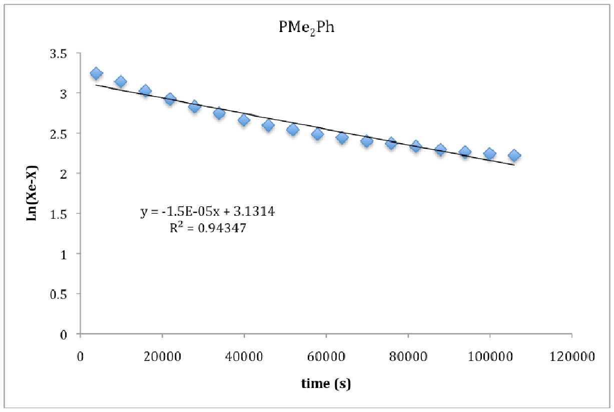

**Figure 6**. Kinetic studies for the conversion of the diastereomers (*R*)-**2** to (*S*)-**2** in the presence of $PMe_2Ph$ (1 M) in $C_6D_6$ followed by $^1$H NMR spectroscopy at 40 °C. ($X_e$ is the equilibrium

concentration of (*S*)-**2**, while X is the increasing concentration of (*S*)-**2** with time.)

**Variable Temperature NMR Studies**

$PMe_3$ (4 μL, 0.038 mmol, 2 equiv) was added via syringe to a solution of (*S*)-**2** (20 mg, 0.019 mmol, 1 equiv) in $C_7D_8$. After 10 minutes at 22 °C, the reaction mixture was investigated by variable temperature $^1H$ NMR spectroscopy. At -30 °C, three phosphine adducts were observed, (*S*)-**2**($PMe_3$) ($\delta H_\alpha$ = 15.51 ppm, $J_{CH}$ = 121 Hz, $J_{HP}$ = 5 Hz), (*S*)-**2'**($PMe_3$) (~20% of total (*S*) adduct; $\delta H_\alpha$ = 13.94 ppm, $J_{HP}$ = 6 Hz), and (*R*)-**2**($PMe_3$) ($\delta H_\alpha$ = 13.83 ppm, $J_{CH}$ = 122 Hz, $J_{HP}$ = 7 Hz), along with (*S*)-**2** and (*R*)-**2** (Figure 7).

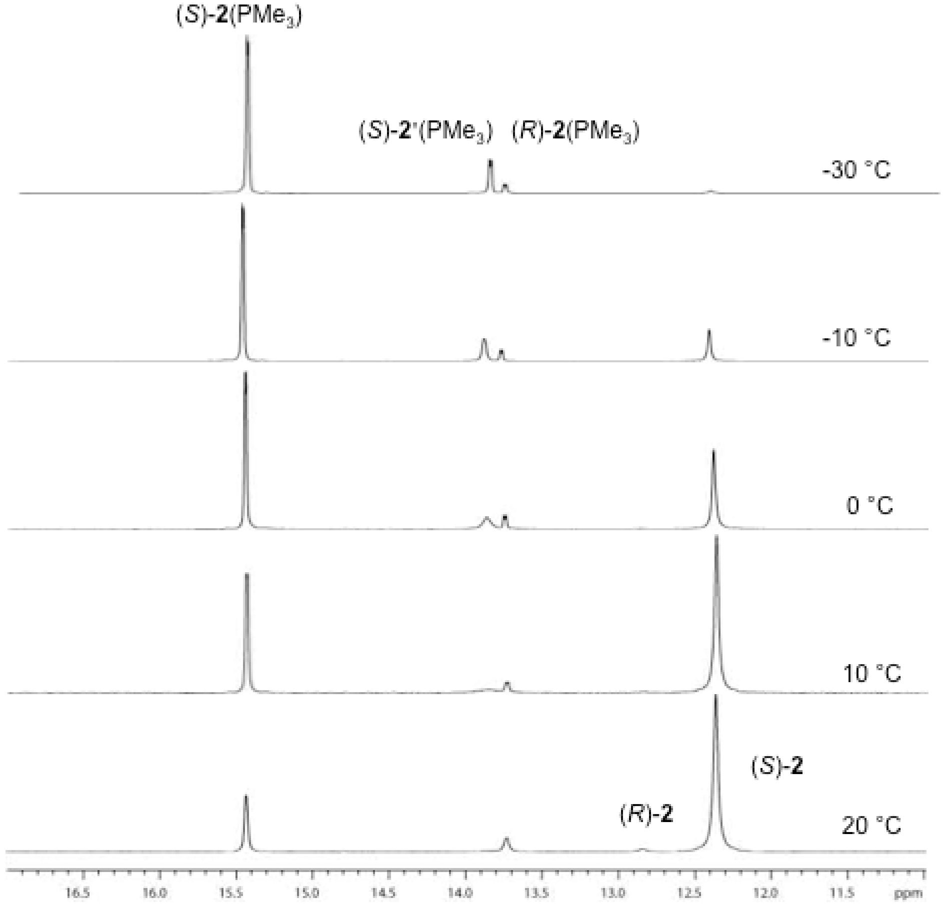

**Figure 7.** Variable temperature 500 MHz $^1H$ NMR spectroscopic studies of the reaction mixture after 10 minutes at 22 °C.

The reaction mixture was allowed to warm up to room temperature. After ~6 h at 22 °C, the reaction mixture was investigated again by variable temperature $^1H$ (Figure 8) and $^{31}P$

(Figure 9) NMR spectroscopy. At -30 °C, four phosphine adducts were observed: (*S*)-**2**($PMe_3$) ($\delta H_\alpha = 15.51$ ppm, $J_{CH} = 121$ Hz, $J_{HP} = 5$ Hz; $\delta P_\alpha = -8.0$ ppm), (*S*)-**2'**($PMe_3$) (~20% of total (*S*) adduct; $\delta H_\alpha = 13.94$ ppm, $J_{HP} = 6$ Hz; $\delta P_\alpha = -15.9$ ppm), (*R*)-**2'**($PMe_3$) (~5% of total (*R*) adduct; $\delta H_\alpha = 14.86$ ppm, $J_{HP} = 8$ Hz; $\delta P_\alpha = -12.6$ ppm), and (*R*)-**2**($PMe_3$) ($\delta H_\alpha = 13.83$ ppm, $J_{CH} = 122$ Hz, $J_{HP} = 7$ Hz; $\delta P_\alpha = -11.5$ ppm), along with (*S*)-**2** and (*R*)-**2** (observed only in the $^1H$ NMR).

The configurations of (*S*)-**2**($PMe_3$) and (*R*)-**2**($PMe_3$) were established by $^1H$-$^1H$ NOESY experiments at 20 °C and 0.2 s mixing time. Exchange of (*S*)-**2**($PMe_3$) with free (*S*)-**2**, and (*R*)-**2**($PMe_3$) with free (*R*)-**2**, respectively, was observed in the spectrum. The configuration of (*R*)-**2'**($PMe_3$) was established by $^1H$-$^1H$ NOESY experiments at 40 °C and 0.5 s mixing time. Exchange of (*R*)-**2'**($PMe_3$) with free (*R*)-**2** was observed in the spectrum. The configuration of (*S*)-**2'**($PMe_3$) was established by $^1H$-$^1H$ NOESY experiments at -10 °C and 0.2 s mixing time. Exchange of (*S*)-**2'**($PMe_3$) with (*S*)-**2**($PMe_3$) and free (*S*)-**2** was observed in the spectrum.

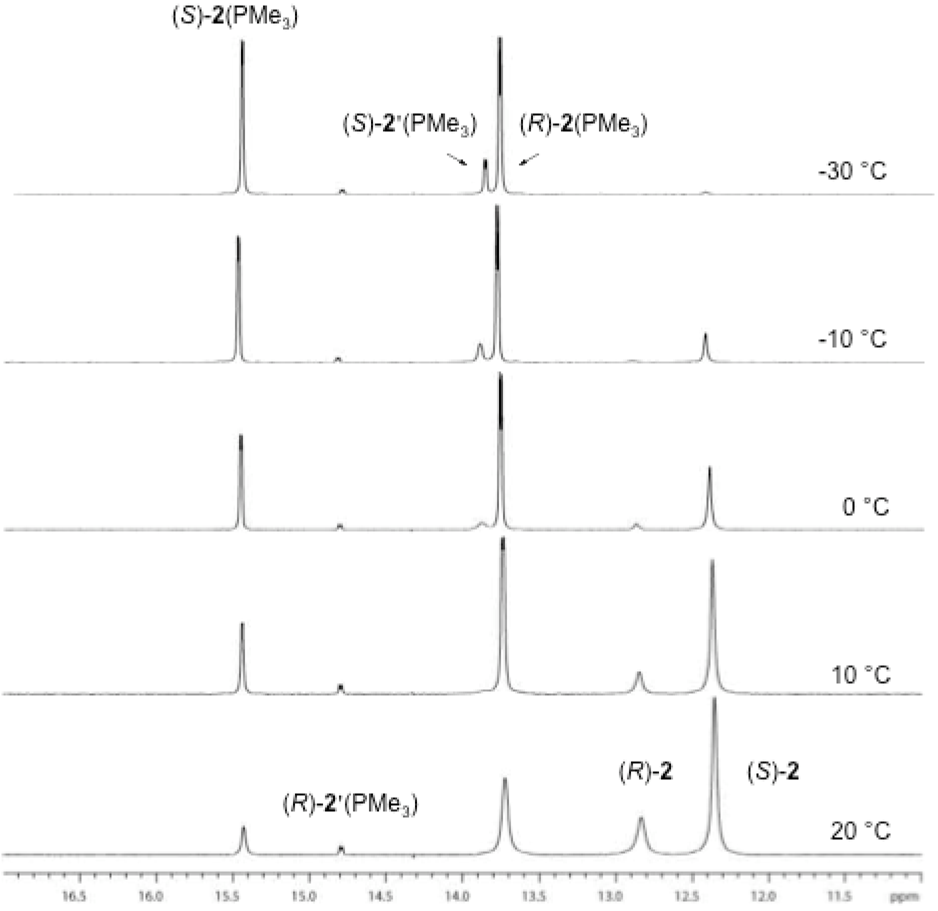

**Figure 8.** Variable temperature 500 MHz $^1$H NMR spectroscopic studies of the reaction mixture after ~6 h at 22 °C.

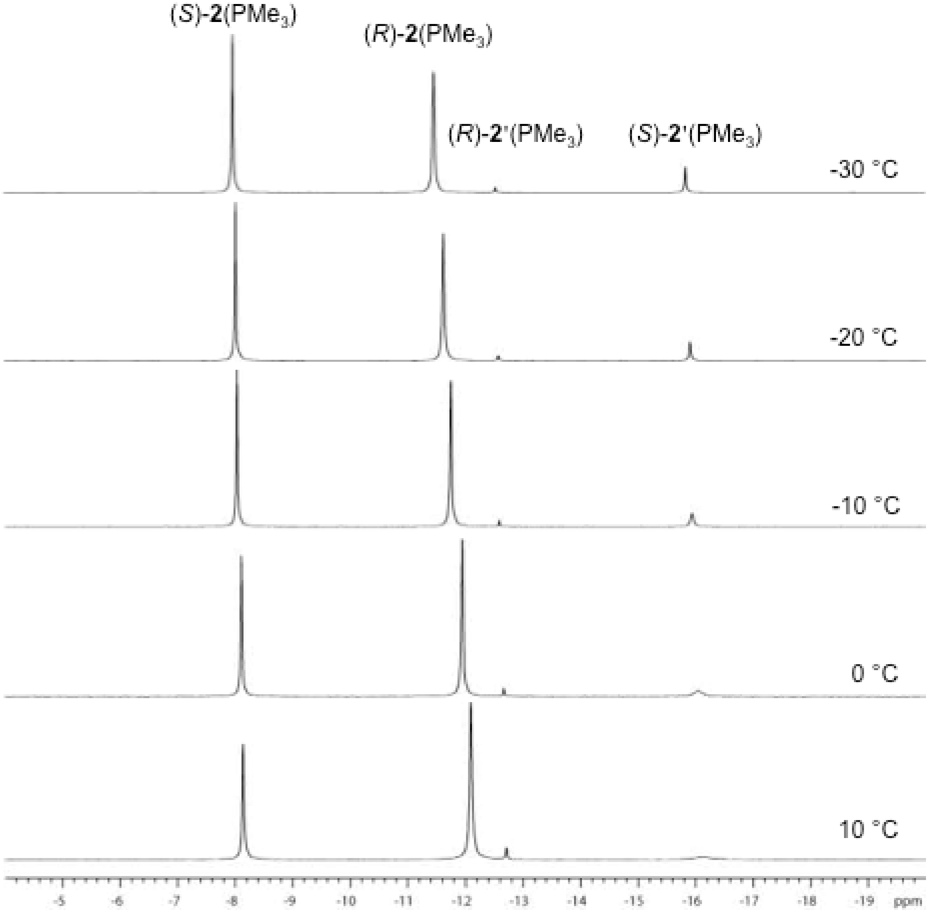

**Figure 9.** Variable temperature 202 MHz $^{31}$P NMR spectroscopic studies of the reaction mixture after ~6 h at 22 °C.

**Synthesis of 2,5-Me$_2$-$^{15}$NC$_4$H$_3$ (40% $^{15}$N).** 2,5-Hexanedione (1.37 mL, 11.6 mmol, 1 equiv) was added via syringe to a solution of $^{15}$NH$_4$OAc (1.0 g, 12.8 mmol, 1.10 equiv) in acetic acid glacial (2 mL) under nitrogen. The reaction mixture was heated at 50 °C for 3 hours. After complete consumption of the starting material, KOH solution was added to neutralize the acetic acid. The organic materials were extracted with diethylether, dried over anhydrous MgSO$_4$ and filtered. The diethylether was evaporated. 2,5-Me$_2$NC$_4$H$_3$ (1.5 mL;14.7 mmol) was added to the reaction mixture, which was distilled under partial vacuum. 2,5-Me$_2$-NC$_4$H$_3$ (40% $^{15}$N) was collected as a colorless liquid (1.29 g, 13.5 mmol, yield = 51%): $^1$H NMR (500 MHz, C$_6$D$_6$) $\delta$

6.34 (br, 0.6H, N*H*), 6.34 (dt, 0.4 H, N*H*, $J_{HN}$ = 93.5 Hz, $J_{HH}$ = 2.5 Hz), 5.94 (d, 2H, C*H*, $J_{HH}$ = 2.5 Hz), 1.94 (s, 6H, C$H_3$); $^{15}$N NMR (50 MHz, $C_6D_6$) δ 153.

**Mo(NAr)(CHCMe$_2$Ph)(2,5-Me$_2$$^{15}$NC$_4$H$_2$)$_2$.** The same procedure as the one used for the preparation of the non-labeled Mo(NAr)(CHCMe$_2$Ph)(2,5-Me$_2$NC$_4$H$_2$)$_2$.[v] $^{15}$N NMR (50 MHz, $CD_2Cl_2$, -30 °C) δ 262, 190.

**Mo(NAr)(CHCMe$_2$Ph)(2,5-Me$_2$$^{15}$NC$_4$H$_2$)(1).** The same procedure as the one used for the preparation of the non-labeled Mo(NAr)(CHCMe$_2$Ph)(2,5-Me$_2$NC$_4$H$_2$)(**1**).[ii] After recrystallization from pentane red crystals of pure (*S*)-**2** (40% $^{15}$N label) were obtained (yield = 70%): $^{15}$N NMR (50 MHz, $C_6D_6$) δ 231.

## $^{31}$P Variable Temperature NMR Studies of the $^{15}$N-labeled (40%) Analogs

PMe$_3$ (10 μL, 0.094 mmol, 2 equiv) was added via syringe to a solution of 40% $^{15}$N-labeled (*S*)-**2** (50 mg, 0.047 mmol, 1 equiv) in $C_7D_8$. After 3h at 22 °C, the reaction mixture was investigated by variable temperature $^{31}$P NMR spectroscopy. At -30 °C, four phosphine adducts were observed: (*S*)-**2**(PMe$_3$) ($\delta P_\alpha$ = -8.0 ppm, $J_{PN}$ = 24.1 Hz), (*S*)-**2'**(PMe$_3$) (~20% of total (*S*) adduct; $\delta P_\alpha$ = -15.9 ppm, $J_{PN}$ = 26.5 Hz), (*R*)-**2'**(PMe$_3$) (~5% of total (*R*) adduct; $\delta P_\alpha$ = -12.6 ppm, $J_{PN}$ = 31.6 Hz), and (*R*)-**2**(PMe$_3$) ($\delta P_\alpha$ = -11.5 ppm, $J_{PN}$ = 26.5 Hz) (Figure 10).

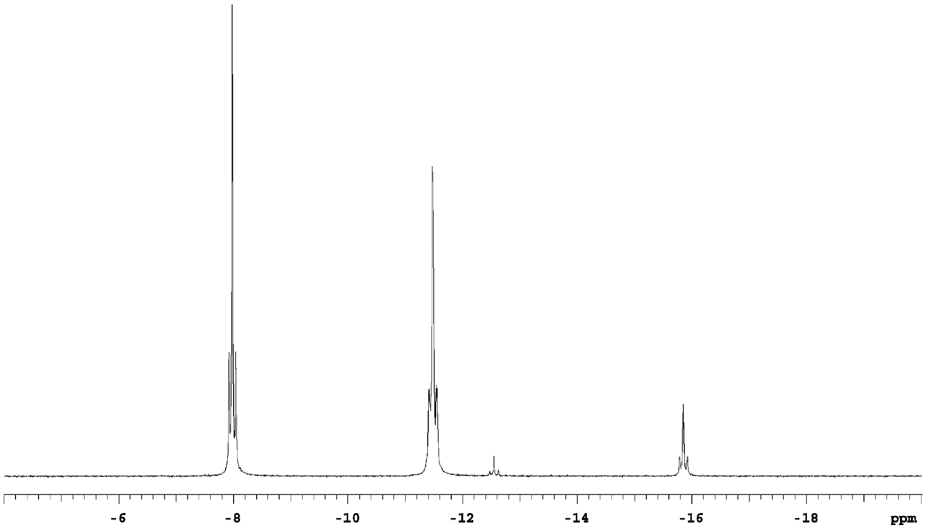

**Figure 10.** 202 MHz $^{31}P$ NMR spectrum at -30 °C of the $^{15}N$-labeled (40%) analogs.

**Mo(NAr)($^{13}$CHCMe$_3$)(2,5-Me$_2$NC$_4$H$_2$)(1).** The same procedure as the one used for the preparation of Mo(NAr)(CHCMe$_2$Ph)(2,5-Me$_2$NC$_4$H$_2$)(**1**).[ii] After recrystallization from tetramethysilane orange crystals of pure diastereomer were obtained. $^1H$ NMR (500 MHz, $C_7D_8$) selected peak δ 12.29 (d, 1H, *syn* Mo=$^{13}$C*H*, $J_{CH}$ = 117 Hz); $^{13}C$ NMR (125 MHz, $C_7D_8$) selected peak δ 295.5 (Mo=$^{13}$*C*H).

## $^1$H Variable Temperature NMR Studies of the $^{13}$C-labeled Analogs

PMe$_3$ (4 μL, 0.038 mmol, 2 equiv) was added via syringe to a solution of Mo(NAr)($^{13}$CHCMe$_3$)(2,5-Me$_2$NC$_4$H$_2$)(**1**) (19 mg, 0.019 mmol, 1 equiv) in $C_7D_8$. After 3h at 22 °C, the reaction mixture was investigated by variable temperature $^1H$ (Figure 11), $^{13}C$ (Figure 12), and $^{31}P$ (Figure 13) NMR spectroscopy. At -30 °C, four phosphine adducts were observed: (*S*)-**2**(PMe$_3$) ($\delta H_\alpha$ = 15.45 ppm, $J_{CH}$ = 122 Hz, $J_{HP}$ = 4 Hz; $\delta P_\alpha$ = -7.2 ppm, $J_{CP}$ = 17 Hz; $\delta C_\alpha$ = 310.7 ppm), (*S*)-**2'**(PMe$_3$) (~20% of total (*S*) adduct; $\delta H_\alpha$ = 13.83 ppm, $J_{CH}$ = 120 Hz, $J_{HP}$ = 5 Hz; $\delta P_\alpha$ = -17.5 ppm, $J_{CP}$ = 19 Hz; $\delta C_\alpha$ = 308.8 ppm), (*R*)-**2'**(PMe$_3$) (~5% of total (*R*) adduct; $\delta H_\alpha$ = 15.51 ppm, $J_{CH}$ = 143 Hz, $J_{HP}$ = 7 Hz; $\delta P_\alpha$ = -12.3 ppm, $J_{CP}$ = 19 Hz; $\delta C_\alpha$ = 332.3 ppm), and (*R*)-**2**(PMe$_3$) ($\delta H_\alpha$ = 13.41 ppm, $J_{CH}$ = 122 Hz, $J_{HP}$ = 6 Hz; $\delta P_\alpha$ = -11.3 ppm, $J_{CP}$ = 19 Hz; $\delta C_\alpha$ = 311.4 ppm), along with (*S*)-**2** and (*R*)-**2** (observed only in the $^1H$ and $^{13}C$ NMRs).

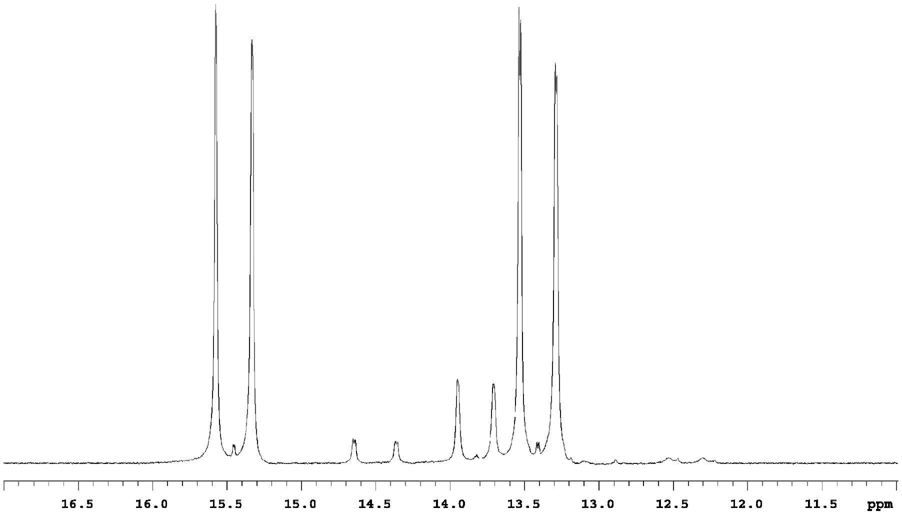

**Figure 11.** 500 MHz $^1$H NMR spectrum at -30 °C of the $^{13}$C-labeled analogs.

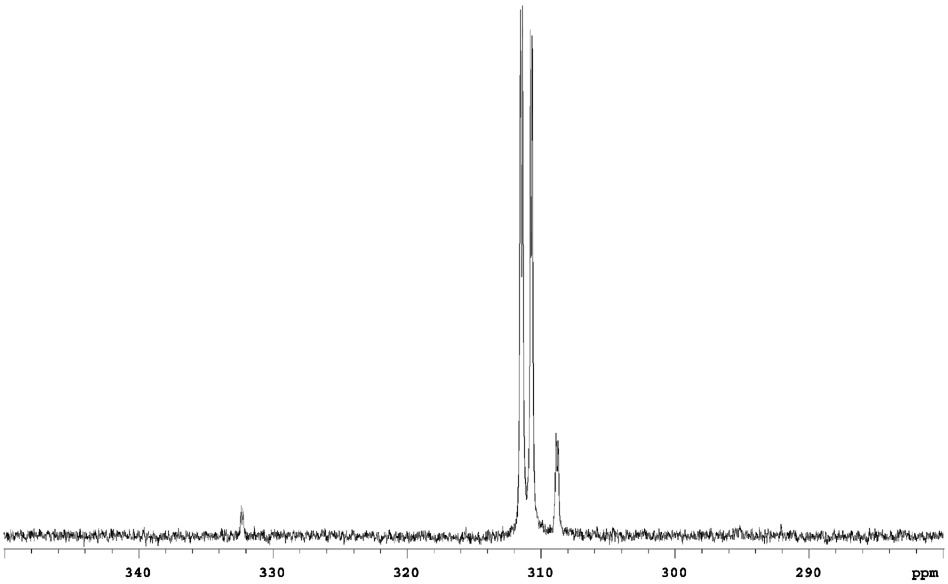

**Figure 12.** 125 MHz $^{13}$C NMR spectrum at -30 °C of the $^{13}$C-labeled analogs.

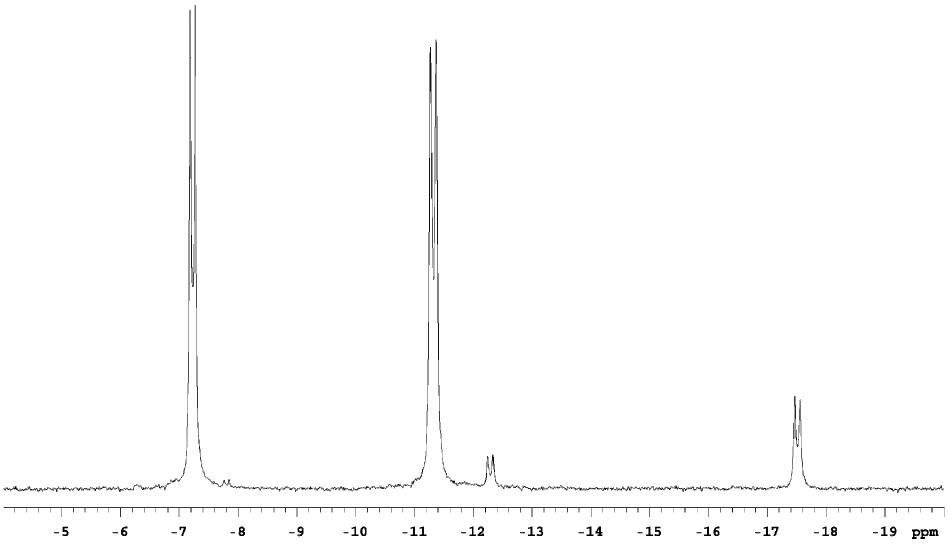

**Figure 13.** 202 MHz $^{31}$P NMR spectrum at -30 °C of the $^{13}$C-labeled analogs.

**(*S*)- and (*R*)- Mo(NAr)($CH_2$)($Me_2$Pyr)(1).** Ethylene (1 equiv) was added to a solution of (*S*)-**2** (25.5 mg, 1 equiv) in $C_7D_8$ (40 mM). The $^1H$ NMR was recorded after 5 minutes at 10 °C. The two methylidenes are observed in the ratio of 2:1. $^1H$ NMR (500 MHz, $C_7D_8$, 10 °C) selected peaks δ 67% $\delta H_\alpha$ = 12.35 (d, 1H, Mo=C*H*, $J_{HH}$ = 4.5 Hz), 12.13 (d, 1H, Mo=C*H*, $J_{HH}$ = 4.5 Hz); 33% at 10 °C, $\delta H_\alpha$ = 12.94 (d, 1H, Mo=C*H*, $J_{HH}$ = 4.0 Hz), 12.24 (d, 1H, Mo=C*H*, $J_{HH}$ = 4.0 Hz); When $^{13}C_2H_4$ was used, the following $^{13}C$ NMR was observed. $^{13}C$ NMR (125 MHz, $C_7D_8$, 10 °C) selected peaks δ 276.3 (Mo=*C*$H_2$), 275.9 (Mo=*C*$H_2$).

**Mo(NAr)($CH_2CH_2CH_2$)($Me_2Pyr$)(1).** Ethylene (1 atm) was added to a solution of (*S*)-**2** (25.5 mg) in $C_7D_8$ (40 mM). At 22 °C, (*S*)- and (*R*)- Mo(NAr)($CH_2$)($Me_2Pyr$)(**1**), and Mo(NAr)($CH_2CH_2CH_2$)($Me_2Pyr$)(**1**) interconvert readily on the NMR time scale through gain and loss of ethylene, respectively. The reaction mixture was allowed to cool down to -70 °C. Only Mo(NAr)($CH_2CH_2CH_2$)($Me_2Pyr$)(**1**) was observed by $^1H$ NMR spectroscopy. $^1H$ NMR (500 MHz, $C_7D_8$, -70 °C) selected peaks $\delta H_\alpha$ = 6.16, 5.69, 5.24, 5.03; $\delta H_\beta$ = 0.74, -0.16. When $^{13}C_2H_4$ was used, the following $^{13}C$ NMR was observed. $^{13}C$ NMR (125 MHz, $C_7D_8$, -70 °C) selected peaks $\delta C_\alpha$ = 102.2, 101.2; $\delta C_\beta$ = -1.1.

*X-ray Crystallographic Procedure.*

Selected single crystals of (R)-**2**($PMe_3$)·0.5($C_5H_{12}$)·0.25($PC_3H_9$), [$C_{57}H_{79}Br_2MoN_2O_2PSi$]·0.5($C_5H_{12}$)·0.25($PC_3H_9$), suitable for X-ray crystallography were used for structural determination. The X-ray intensity data were measured at 100(2) K (Oxford Cryostream 700) on a Bruker APEX CCD-based 3-circle platform X-ray diffractometer system equipped with a Mo-target X-ray tube ($\lambda$ = 0.71073 Å) operated at 2000 W power. The crystals were mounted on a goniometer head with paratone oil. The detector was placed at a distance of 6.00 cm from the crystal. For each experiment a total of 2400 frames were collected with a scan width of 0.3° in $\omega$ and an exposure time of 20 s/frame. The frames were integrated with the Bruker SAINT software package using a narrow-frame integration algorithm to a maximum $2\theta$ angle of 56.54° (0.75 Å resolution). The final cell constants are based upon the refinement of the XYZ-centroids of several thousand reflections above $20\sigma(I)$. Analysis of the data showed negligible decay during data collection. Data were corrected for absorption effects using the empirical method (SADABS). The structures were solved by direct methods and refined by full-matrix least squares procedures on $|F^2|$ using the Bruker SHELXTL (version 6.14) software package. The coordinates of heavy atoms for the structures were found in direct method *E* maps. The remaining atoms were located after an alternative series of least-squares cycles and difference Fourier maps. All hydrogen atoms were included in idealized positions for structure factor calculations. Anisotropic displacement parameters were assigned to all non-hydrogen atoms, except those in the solvent molecules.

Complex (R)-**2**($PMe_3$) crystallized in orthorhombic space group $P2_12_12_1$ with one molecule in the asymmetric unit. Many atoms in the ligand **1** appeared to be disordered over two orientations. The atomic positions of the two components are found to be relative close, indicating structural flexibility of the ligand. The disorder was modeled individually in each case and refined with the help of similarity restraints on 1-2 and 1-3 distances and displacement parameters as well as rigid bond restraints for anisotropic displacement parameters. In addition, a mixture of solvent molecules was found to fill the voids in the packing of (R)-**2**($PMe_3$). The mixture was refined as pentane and trimethylphosphine with partial occupancy of 0.5 and 0.25, respectively, which results in noninteger values for the elements C, H, and P in the calculated empirical formula of the structure of (R)-**2**($PMe_3$)**.** The overlapping of pentane and trimethylphosphine molecules in the asymmetric unit suggests statistical distribution of the two solvent molecules.

Relevant crystallographic data are summarized in Table 1. The cif file is available.

**Table 1**.  Crystal data and structure refinement for (*R*)-**2**(PMe$_3$).

| | | |
|---|---|---|
| Identification code | [$C_{57}H_{79}Br_2MoN_2O_2PSi$]0.5($C_5H_{12}$)0.25($PC_3H_9$) | |
| Empirical formula | $C_{60.25}H_{87.25}Br_2MoN_2O_2P_{1.25}Si$ | |
| Formula weight | 1194.13 | |
| Temperature | 100(2) K | |
| Wavelength | 0.71073 Å | |
| Crystal system | Orthorhombic | |
| Space group | $P2_12_12_1$ | |
| Unit cell dimensions | a = 10.8412(15) Å | $\alpha$= 90° |
| | b = 18.736(3) Å | $\beta$= 90° |
| | c = 29.809(4) Å | $\gamma$ = 90° |
| Volume | 6054.7(15) Å$^3$ | |
| Z | 4 | |
| Density (calculated) | 1.310 Mg/m$^3$ | |
| Absorption coefficient | 1.630 mm$^{-1}$ | |
| F(000) | 2494 | |
| Crystal size | 0.10 x 0.09 x 0.08 mm$^3$ | |
| Theta range for data collection | 2.00 to 26.00° | |
| Index ranges | -13<=h<=13, -23<=k<=23, -36<=l<=36 | |
| Reflections collected | 96274 | |
| Independent reflections | 11897 [R(int) = 0.0413] | |
| Completeness to theta = 26.00∞ | 99.9 % | |
| Absorption correction | Semi-empirical from equivalents | |
| Max. and min. transmission | 0.8807 and 0.8540 | |
| Refinement method | Full-matrix least-squares on F$^2$ | |
| Data / restraints / parameters | 11897 / 899 / 736 | |
| Goodness-of-fit on F$^2$ | 1.047 | |
| Final R indices [I>2sigma(I)] | R1 = 0.0401, wR2 = 0.1015 | |
| R indices (all data) | R1 = 0.0448, wR2 = 0.1047 | |
| Absolute structure parameter | 0.000(8) | |
| Extinction coefficient | na | |
| Largest diff. peak and hole | 0.860 and -0.522 e.Å$^{-3}$ | |

**References**

---

[i] Binsch, G.; Lambert, J. B.; Roberts, B. W.; Roberts, J. D. *J. Am. Chem. Soc.* **1964**, *86*, 5564.

[ii] Malcolmson, S. J.; Meek, S. J.; Sattely, E. S.; Schrock, R. R.; Hoveyda, A. H. *Nature*, in press.

[iii] Meek, S. J.; Malcolmson, S. J.; Li, B.; Schrock, R. R.; Hoveyda, A. H., unpublished results.

[iv] Sinha A. *Ph. D. Thesis*, Massachusetts Institute of Technology, **2006**.

[v] Singh, R.; Czekelius, C.; Schrock, R. R.; Müller, P.; Hoveyda, A. H. *Organometallics* **2007**, *26*, 2528.